Inorg. Chem. **2006**, *45*, 4791−4800

Molybdenum and Tungsten η^2-Alkyne-1-thio Complexes Acting as Sulfur Donors in Homoleptic Werner Type Complexes with Nickel(II) and Palladium(II)

Wolfram W. Seidel,* Maria D. Ibarra Arias, Markus Schaffrath, Mareike C. Jahnke, Alexander Hepp, and Tania Pape

Institut für Anorganische und Analytische Chemie, Westfälische Wilhelms-Universität Münster, Corrensstrasse 30/36, 48149 Münster, Germany

Received December 22, 2005

Facile access to the η^2-alkyne-1-thio complexes [Tp′M(CO)$_2${η^2-(BnS)CC(S)}] (Tp′ = hydrotris(3,5-dimethylpyrazolyl)-borate; Bn = benzyl; M = Mo, W) by reductive removal of one benzyl group in the corresponding bis(benzylthio)-acetylene complexes, [Tp′M(CO)$_2${η^2-(BnS)CC(SBn)}](PF$_6$), has been thoroughly investigated. Experimental evidence of the intermediates, [Tp′M(CO)$_2${η^2-(BnS)CC(SBn)}] (M = Mo, W), and the fate of the cleaved benzyl group by isolation of the byproduct, [Tp′W(CO){C(O)Bn}{η^2-(BnS)CC(SBn)}], is provided. Neutral η^2-alkyne-1-thio complexes [Tp′M(CO)$_2${η^2-(BnS)CC(S)}] bearing a free terminal sulfur atom have been established as monodentate ligands L in homoleptic pentanuclear [M′L$_4$]$^{2+}$ complexes with nickel(II) and palladium(II). Comparison of the NMR and IR spectroscopic as well as cyclovoltammetric data of the heterobimetallic complexes with the free thio-alkyne complexes reveals a strong electronic coupling of the redox-active η^2-*CC*-bound metal centers and the sulfur-coordinated metal ion.

Introduction

Cooperative phenomena between two or more electronically related metal ions are attracting enormous attention in current coordination chemical research. The continuing interest can be attributed to the fact that metallo-enzyme activity is frequently based on bimetallic reactivity patterns. The profound understanding of electronic and magnetic exchange interactions through or across different bridging ligands is fundamental to the search for cooperative reactivity. Our approach is directed toward linkage of organometallic complex centers with predominantly sulfur-coordinated metal ions. This can be achieved by the use of either alkyne-1-thiolato or alkyne-1,2-dithiolato ligands, which can bind one metal center by the triple bond and the other by coordination through sulfur donor atoms. In contrast to the more-rigid sulfide bridging of two metal centers, the η^2-*CC*−η^1-*S* linkage by an alkyne-1-thiolato unit leads to bimetallic complexes with more structural flexibility. Additionally, the approach establishes a general method for combining several organometallic components with a variety of Werner type complexes because of the high degree of metal discrimination of the two different donors.

First reports on alkyne-1-thiolato ligands indicated the tendency of sulfur to govern the coordination behavior even in the formation of dinuclear complexes.[1−3] Bis(alkyne-thiolato)titanocene complexes, for example, have been shown to bind Ni(0) at the sulfur atoms and not at the triple bond.[4] Additionally, some investigations disclosed the propensity of alkyne−sulfur bonds to cleave in the coordination sphere of metal complexes.[5−7] Therefore, our approach is directed at the preceding formation of stable four-electron-donor alkyne complexes with bis(benzylthio)acetylene and subsequent reductive removal of the benzyl groups in the complex.

* To whom correspondence should be addressed. E-mail: seidelww@uni-muenster.de.

(1) Weigand, W. *Z. Naturforsch.* **1991**, *46b*, 1333−1337.
(2) Weigand, W.; Weishäupl, M.; Robl, C. *Z. Naturforsch.* **1996**, *51b*, 501−505.
(3) Ara, I.; Delgado, E.; Fornies, J.; Hernandes, E.; Lalinde, E.; Mansilla, N.; Moreno, M. T. *J. Chem. Soc., Dalton Trans.* **1998**, 3199−3208.
(4) Sugiyama, H.; Hayashi, Y.; Kawaguchi, H.; Tatsumi, K. *Inorg. Chem.* **1998**, *37*, 6773−6779.
(5) Weigand, W.; Robl, C. *Chem. Ber.* **1993**, *126*, 1807−1809.
(6) Alcalde, M. I.; Carty, A. J.; Chi, Y.; Delgado, E.; Donnadieu, B.; Hernandez, E.; Dallmann, K.; Sanches-Nieves, J. *J. Chem. Soc., Dalton Trans.* **2001**, 2502−2507.
(7) Sunada, Y.; Hayashi, Y.; Kawaguchi, H.; Tatsumi, K. *Inorg. Chem.* **2001**, *40*, 7072−7078.

10.1021/ic052178y CCC: $33.50
Published on Web 05/17/2006

Chart 1

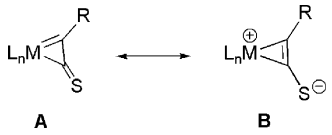

The resulting metal-stabilized alkynethiolates can finally be reacted with thiophilic transition-metal ions. Connor and Angelici demonstrated that the coordination behavior of bis-(methylthio)acetylene is determined by the triple bond and that heterobimetallic complexes are accessible by subsequent sulfide coordination.[8,9] However, depending on the particular metal center, the sulfide function can compete as a donor and the alkyne−sulfur bond is likewise sensitive to bond cleavage.[10]

Alkyne complexes with a terminal sulfur atom have been synthesized in W(II) and Mo(II) complexes by coupling of either intermediate carbyne and CS ligands[11,12] or carbyne and CO ligands and subsequent reaction with Lawesson's reagent.[13] The η^2-*CC* binding in the resulting thio-alkyne complexes is best described by superposition of two resonance forms underlining either the thioketenyl character (Chart I, form A) or the rather zwitterionic alkyne complex form (Chart I, form B). However, the nucleophilicity at the sulfur atom, which is particularly evident in form B, has not been explored with regard to coordination chemistry.

We have recently reported on a heterodinuclear complex of [Tp′W(CO)$_2${η^2-(BnS)CC(S)}] (Tp′ = hydrotris(3,5-dimethylpyrazolyl)borate, Bn = benzyl hereafter) with Cu(I) that exhibits the η^2-*CC* −η^1-*S* bridging mode of an alkyne-1-thio ligand.[14] Herein, we report on cationic bis(benzylthio)-acetylene complexes and neutral η^2-*CC*-alkyne-1-thio complexes with the [Tp′M(CO)$_2$] fragment (M = Mo^{II}, W^{II}), comprising a thorough investigation of the conversion reaction and disclosure of the unexpected fate of the cleaved benzyl group. Finally, we give an account of the coordination behavior of [Tp′M(CO)$_2${η^2-(BnS)CC(S)}] (M = Mo, W) with Ni(II) and Pd(II). We present molecular structures in the solid state at each level of the synthetic scheme, NMR analyses regarding the dynamic behavior of the η^2-*CC*-alkyne-1-thio complexes in solution, and electrochemical studies with the heterobimetallic pentanuclear [Tp′M(CO)$_2$-{η^2-(BnS)CC(S)}]$_4$M′(BF$_4$)$_2$ complexes (M = Mo, W; M′ = Ni, Pd).

Experimental Section

General Procedures. All operations were carried out under a dry argon atmosphere using standard Schlenk and glovebox techniques. All solvents were dried and saturated with argon by standard methods and freshly distilled prior to use. PhCH$_2$-SCCSCH$_2$Ph,[15] [Tp′Mo(CO)$_3$],[16] [Tp′W(CO)$_3$][17] (Tp′ = Hydrotris-(3,5-dimethylpyrazolyl)borate), [Ni(CH$_3$CN)$_6$](BF$_4$)$_2$,[18] and C$_8$K[19] were prepared according to literature methods. [Pd(CH$_3$CN)$_4$](BF$_4$)$_2$ was purchased from Aldrich. ^{1}H and ^{13}C NMR spectra were recorded on Bruker AC 200, Bruker Avance 400, and Varian Unity plus 600 NMR spectrometers. Elemental analyses were performed on a Vario EL III CHNS elemental analyzer. ESI mass spectra were obtained using a QUATTRO LCZ (Waters-Micromass). Infrared spectra were recorded on a Bruker Vector 22 and UV−vis spectra on a Cary 50 Varian spectrophotometer. Cyclic voltammograms were acquired on an ECO/Metrohm PGSTAT 30 potentiostat using a glassy carbon working electrode, a Ag/0.01 M AgNO$_3$/CH$_3$CN reference electrode, (NBu$_4$)(PF$_6$) as the supporting electrolyte, and ferrocene as the internal standard.

[Tp′Mo(CO)$_2${η^2-(BnS)CC(SBn)}](PF$_6$) 1a. A solution of 6.92 g (14.5 mmol) of [Tp′Mo(CO)$_3$] and 3.92 g (14.5 mmol) of bis-(benzylthio)acetylene in 150 mL of dichloromethane was treated with 4.8 g (14.5 mmol) of [(C$_5$H$_5$)$_2$Fe](PF$_6$). CO evolution was observed while the solution turned dark green. After 3 h, the solvent was removed in vacuo, and the residue was washed three times with 50 mL of diethyl ether. The residue was dissolved again in 60 mL of dichloromethane and filtered through a Celite pad. **1a** was crystallized by diffusion of diethyl ether into a solution of the complex in dichloromethane. Yield: 8.7 g (10 mmol, 69%), olive crystals. ^{1}H NMR (CDCl$_3$): δ 7.41−7.28 (m, 8 H, Ph-*H*), 6.88 (m, 2 H, Ph-*H*), 6.03 (s, 3 H, C*H*(CCH$_3$)$_2$), 4.91 (s, 2 H, SC*H*$_2$), 3.11 (s, 2 H, SC*H*$_2$), 2.62 (3 H, C*H*$_3$), 2.51 (6 H, C*H*$_3$), 2.43 (3 H, C*H*$_3$), 1.65 (s, 6 H, C*H*$_3$). ^{13}C NMR (CDCl$_3$): δ 227.0 (Mo*C*SCH$_2$), 215.4 (*C*O), 205.8 (Mo*C*SCH$_2$), 153.5, 151.3, 149.0, 147.0 (*C*CH$_3$), 133.9, 132.3 (Ph-*C*$_{ipso}$), 129.1, 129.0, 128.8, 128.7, 128.6 (Ph-*C*, one resonance is not resolved), 109.3, 107.7 (*C*H(CCH$_3$)$_2$), 44.8, 42.1 (S*C*H$_2$), 15.6, 14.1, 13.0, 12.5 (*C*H$_3$). IR (KBr, cm^{-1}): ν 2051, 2000 (CO), 842 (PF$_6$).

[Tp′W(CO)$_2${η^2-(BnS)CC(SBn)}](PF$_6$) 1b. Tungsten complex **1b** was synthesized by a method analogous to that used for **1a** using 8.2 g (14.5 mmol) of [Tp′W(CO)$_3$]. Yield: 8.9 g (9.34 mmol, 64%), green crystals. ^{1}H NMR (CDCl$_3$): δ 7.42−7.25 (m, 8 H, Ph-*H*), 6.87 (m, 2 H, Ph-*H*), 6.13 (s, 3 H, C*H*(CCH$_3$)$_2$), 4.87 (s, 2 H, SC*H*$_2$), 3.11 (s, 2 H, SC*H*$_2$), 2.65 (s, 3 H, C*H*$_3$), 2.52 (s, 6 H, C*H*$_3$), 2.35 (s, 3 H, C*H*$_3$), 1.80 (s, 6 H, C*H*$_3$). ^{13}C NMR (CDCl$_3$): δ 219.0 ($^1J_{WC}$ = 50 Hz, W*C*SCH$_2$), 213.8 ($^1J_{WC}$ = 137 Hz, W*C*O), 193.6 (W*C*SCH$_2$), 154.8, 152.5, 149.8, 147.2 (*C*CH$_3$), 134.2, 132.7 (Ph-*C*$_{ipso}$), 129.0, 129.0, 128.8, 128.7, 128.6, 128.5 (Ph-*C*), 110.0, 108.2 (*C*H(CCH$_3$)$_2$), 43.6, 41.6 (S*C*H$_2$), 16.2, 14.8, 13.0, 12.4 (*C*H$_3$). IR (KBr, cm^{-1}): ν 2041, 1980 (CO), 840 (PF$_6$).

[Tp′Mo(CO)$_2${η^2-(BnS)CC(S)}] 3a. At −78 °C, 510 mg (3.8 mmol) of C$_8$K was added to a solution of 2.77 g (3.2 mmol) of **1a** in 100 mL of THF. While the solution was stirred for one minute, the color turned from green to red; the formation of **2a** was checked by IR spectroscopy (CO absorptions at 1887 and 1970 cm^{-1}). The solution was heated to 40 °C for approximately 3 days until the disappearance of **2a** was complete, as indicated by IR spectroscopy. The solvent was removed in vacuo, and the product was purified by column chromatography using toluene as eluent. Yellow-brown

(8) Connor, J. A.; Hudson, G. A. *J. Organomet. Chem.* **1978**, *160*, 159−164.
(9) Miller, D. C.; Angelici, R. J. *J. Organomet. Chem.* **1990**, *394*, 235−249.
(10) Miller, D. C.; Angelici, R. J. *Organometallics* **1991**, *10*, 79−89.
(11) Mayr, A.; Lee, T.-Y. *Angew. Chem.* **1993**, *105*, 1835−1837; *Angew. Chem., Int. Ed.* **1993**, *32*, 1726−1728.
(12) Lee, T.-Y.; Mayr, A. *J. Am. Chem. Soc.* **1994**, *116*, 10300−10301.
(13) Hill, A. F.; Malget, J. M.; White, A. J. P.; Williams, D. J. *J. Chem. Soc., Chem. Commun.* **1996**, 721−722.
(14) Seidel, W. W.; Ibarra Arias, M. D.; Schaffrath, M.; Bergander, K. *Dalton Trans.* **2004**, 2053−2054.
(15) Klein, T. R.; Bergemann, M.; Yehia, N. A. M.; Fanghänel, E. *J. Org. Chem.* **1998,** *63*, 4626−4631.
(16) Shiu, K.-B.; Lee, L.-Y. *J. Organomet. Chem.* **1988**, *348*, 357−360.
(17) Philipp, C. C.; White, P. S.; Templeton, J. L. *Inorg. Chem.* **1992**, *31*, 3825−3830.
(18) Heintz, R. A.; Smith, J. A.; Szalay, P. S.; Weisgerber, A.; Dunbar, K. R. *Inorg. Synth.* **2002**, *33*, 75−79.
(19) Cotton, F. A.; Hillard, E. A.; Murillo, C. A.; Wang, X. *Inorg. Chem.* **2003**, *42*, 6063−6070.

crystals of **3a** were obtained by slow evaporation of dichloromethane from a dichloromethane/*n*-hexane solution. Yield: 0.9 g (1.43 mmol, 45%). Anal. Calcd for $C_{26}H_{29}BN_6O_2S_2Mo$: C, 49.69; H, 4.65; N, 13.37. Found: C, 49.43; H, 4.75; N, 13.20. ^{1}H NMR ($CDCl_3$, 213 K): δ (two isomers) 7.41 (m, 1 H, Ph-*H*), 7.40−7.24 (m, 3 H, Ph-*H*), 6.99 (m, 1 H, Ph-*H*), 5.93 (s, 2 H, C*H*(CCH_3)$_2$), 5.82 (s, 1 H, C*H*(CCH_3)$_2$), 5.16 (approximately 1 H, 52% SCH_2), 4.75 (s, br, 1 H, B*H*), 3.26 (approximately 1 H, 48% SCH_2), 2.69 (s, approximately 1.5 H, CH_3), 2.65 (s, approximately 1.5 H, CH_3), 2.47 (s, 3 H, CH_3), 2.42 (s, 3 H, CH_3), 2.37 (s, approximately 1.5 H, CH_3), 2.34 (s, approximately 1.5 H, CH_3), 1.74 (s, 3 H, CH_3), 1.58 (s, 3 H, CH_3). ^{13}C NMR ($CDCl_3$, 213 K): δ (two isomers) 255.5, 251.6 (Mo*C*SCH_2), 227.5, 226.3 (*C*O), 223.7, 222.5 (Mo*C*S), 154.7, 154.5, 151.4, 150.7, 147.0, 146.8, 145.6, 145.2 (*C*CH_3), 137.5, 135.2, 130.1, 129.7, 129.4, 129.2, 128.3, 127.6 (Ph-*C*), 108.6, 108.5, 107.2, 107.0 (*C*H(CCH_3)$_2$), 41.2, 38.7 (S*C*H_2), 16.1, 16.0, 15.0, 14.9, 14.8, 14.7, 13.8, 12.8 (C*C*H_3). IR (KBr, cm^{-1}): ν 2013, 1952 (s, CO). IR (CH_2Cl_2, cm^{-1}): ν 2012, 1941 (s, CO).

[Tp′W(CO)$_2${η^2-(BnS)CC(S)}] 3b and [Tp′W(CO){C(O)Bn}-{η^2-(BnS)CC(SBn)}] 4b. At −78 °C a solution of 3.05 g (3.2 mmol) **1b** in 100 mL THF was treated with 510 mg (3.8 mmol) of C_8K. While the solution was stirred for one minute at −78 °C, the color of the solution turned from green to red, and the formation of **2b** was checked by IR spectroscopy (CO absorptions at 1865 and 1974 cm^{-1}). The solution was warmed to ambient temperature. After 2 h, the disappearance of **2b** was complete, as indicated by IR spectroscopy. The solvent was removed in vacuo, and the product was purified by column chromatography using toluene/THF gradient elution. The less-polar, red product **4b** was eluted first and crystallized from toluene/*n*-hexane. Yield: 720 mg (0.8 mmol, 25%). Yellow-brown crystals of **3b** were obtained by slow evaporation of dichloromethane from dichloromethane/*n*-hexane solution. Yield: 1.1 g (1.54 mmol, 48%).

[Tp′W(CO)$_2${η^2-(BnS)CC(S)}] 3b. Anal. Calcd. for $C_{26}H_{29}BN_6O_2S_2W$: C, 43.59; H, 4.08; N, 11.73. Found: C, 43.42; H, 4.15; N, 11.79. ^{1}H NMR ($CDCl_3$, 213 K): δ (two isomers) 7.42 (m, 1 H, Ph-*H*), 7.28 (m, 3 H, Ph-*H*), 6.95 (m, 1 H, Ph-*H*), 6.00 (s, 2 H, C*H*(CCH_3)$_2$), 5.88 (s, 1 H, C*H*(CCH_3)$_2$), 5.24 (s, approximately 1 H, 52% SCH_2), 4.6 (s, br, 1 H, B*H*), 3.22 (s, approximately 1 H, 48% SCH_2), 2.69 (s, approximately 1.5 H, CH_3), 2.65 (s, approximately 1.5 H, CH_3), 2.50 (s, 3 H, CH_3), 2.46 (s, 3 H, CH_3), 2.38 (s, approximately 1.5 H, CH_3), 2.35 (s, approximately 1.5 H, CH_3), 1.88 (s, 3 H, CH_3), 1.73 (s, 3 H, CH_3). ^{13}C NMR ($CDCl_3$, 213 K): δ 237.6, 232.7 (WCSCH_2), 220.7, 219.3 (W*C*O), 214.3, 213.8 (W*C*S), 154.9, 154.7, 151.8, 151.0, 146.6, 146.4, 144.9, 144.5 (*C*CH_3), 137.1, 134.8, 129.3, 128.8, 128.5, 128.4, 127.4, 126.9 (Ph-*C*), 108.3, 108.2, 106.7, 106.6 (*C*H(CCH_3)$_2$), 39.7, 36.2 (S*C*H_2), 15.9, 15.8, 14.9, 14.7, 13.1, 13.0, 12.8, 12.7 (*C*H_3). IR (KBr, cm^{-1}): ν 1995, 1924 (s, CO). IR (CH_2Cl_2, cm^{-1}): ν 2004, 1925 (s, CO).

[Tp′W(CO){C(O)Bn}{η^2-(BnS)CC(SBn)}] 4b. Anal. Calcd. for $C_{40}H_{43}BN_6O_2S_2W$: C, 53.46; H, 4.82; N, 9.35. Found: C, 53.60; H, 5.03; N, 9.23. ^{1}H NMR (C_6D_6): δ 7.66 (d, 2 H, Ph-*H*), 7.39−6.80 (m, 13 H, Ph-*H*), 5.68 (s, 1 H, C*H*), 5.49 (s, 1 H, C*H*), 5.39 (s, 1 H, C*H*), 4.84 (d, 1 H, C*H*H, ^2J = 12.7 Hz), 4.72 (d, 1 H, C*H*H, ^2J = 12.7 Hz), 4.15 (d, 1 H, C*H*H, ^2J = 13.3 Hz), 3.56 (d, 1 H, C*H*H, ^2J = 13.3 Hz), 3.84 (d, 1 H, C*H*H, ^2J = 12.1 Hz), 3.15 (d, 1 H, C*H*H, ^2J = 12.1 Hz), 2.40 (s, 3 H, CH_3), 2.32 (s, 3 H, CH_3), 2.11 (s, 3 H, CH_3), 2.07 (s, 3 H, CH_3), 1.93 (s, 3 H, CH_3), 1.86 (s, 3 H, CH_3). ^{13}C NMR ($CDCl_3$): δ 285.6 (W*C*(O)Bn), 239.4 (WCSCH_2), 205.2 (*C*O), 196.5 (WCSCH_2), 153.5, 153.3, 150.3, 144.3, 137.5, 136.4 (*C*CH_3), 130.2−124.8 (12 Ph-*C*), 107.8, 107.2, 106.7 (*C*H), 70.9 (C(O)*C*H_2Ph), 40.8, 40.6 (S*C*H_2Ph), 16.3, 16.2, 15.1, 12.8, 12.7, 12.2 (*C*H_3). IR (KBr, cm^{-1}): ν 1899 (s, CO), 1576 (m, BnCO). IR (THF, cm^{-1}): ν 1923 (s, CO), 1574 (m, BnCO).

[{Tp′(CO)$_2$Mo-η^2-(BnS)CC(S)}$_4$Ni](BF$_4$)$_2$ 5a. Under strict anaerobic conditions, 150 mg of **3a** (0.24 mmol) was added to a solution of 29 mg (0.06 mmol) of [Ni(CH_3CN)$_6$](BF_4)$_2$ in 15 mL of dichloromethane. The light blue solution of [Ni(CH_3CN)$_6$](BF_4)$_2$ turned red immediately, and the complex formation was checked by IR spectroscopy. After 1 h of being stirred, the solution was reduced in volume and complex **5a** was isolated by gas-phase diffusion of diethyl ether in a dichloromethane solution of **5a**. Yield: 155 mg (93%), red solid. ^{1}H NMR ($CDCl_3$): δ 7.31 (m, 12 H, Ph-*H*), 6.90 (m, 8 H, Ph-*H*), 5.96 (s, 4 H, C*H*(CCH_3)$_2$), 5.90 (s, 8 H, C*H*(CCH_3)$_2$), 4.84 (s, br, 4 H, B*H*), 3.21 (s, 8 H, SCH_2), 2.55 (s, 12 H, CH_3), 2.48 (s, 24 H, CH_3), 2.38 (s, 12 H, CH_3), 1.53 (s, 24 H, CH_3). ^{13}C NMR ($CDCl_3$): δ 238.3 (Mo*C*SCH_2), 219.5 (*C*O), 219.2 (Mo*C*SNi), 153.5, 151.4, 147.8, 146.2 (*C*CH_3), 134.2, 129.1, 129.0, 128.3 (Ph-*C*), 108.7, 107.2 (*C*H(CCH_3)$_2$), 41.2 (S*C*H_2), 15.5, 14.2, 13.0, 12.7 (*C*H_3). IR (CH_2Cl_2, cm^{-1}): ν 2038, 1976 (s, CO).

[{Tp′(CO)$_2$W-η^2-(BnS)CC(S)}$_4$Ni](BF$_4$)$_2$ 5b. The corresponding tungsten complex **5b** was synthesized by a method analogous to that used for **5a** using 173 mg (0.24 mmol) of **3b**. Yield: 165 mg (88%), red solid. ^{1}H NMR ($CDCl_3$): δ 7.25 (m, 12 H, Ph-*H*), 6.86 (m, 8 H, Ph-*H*), 6.00 (s, 4 H, C*H*(CCH_3)$_2$), 5.91 (s, 8 H, C*H*(CCH_3)$_2$), 4.77 (s, br, 4 H, B*H*), 3.16 (s, 8 H, SCH_2), 2.56 (s, 12 H, CH_3), 2.47 (s, 24 H, CH_3), 2.35 (s, 12 H, CH_3), 1.65 (s, 24 H, CH_3). ^{13}C NMR ($CDCl_3$): δ 227.0 (W*C*SCH_2), 217.3 (*C*O), 207.4 (W*C*SNi), 154.8, 152.6, 148.2, 146.0 (*C*CH_3), 134.7, 128.7, 128.6, 127.8 (Ph-*C*), 109.1, 107.4 (*C*H(CCH_3)$_2$), 40.9 (S*C*H_2), 15.9, 14.9, 12.9, 12.5 (*C*H_3). IR (CH_2Cl_2, cm^{-1}): ν 2027, 1955 (s, CO).

[{Tp′(CO)$_2$Mo-η^2-(BnS)CC(S)}$_4$Pd](BF$_4$)$_2$ 6a. Under strict anaerobic conditions, 19 mg (0.05 mmol) of [Pd(CH_3CN)$_4$](BF_4)$_2$ was added to a solution of 123 mg (0.2 mmol) of **3a** in 15 mL of dichloromethane. Immediately, the yellow-green solution of **3a** turned red, and the complex formation was checked by IR spectroscopy. After 12 h of being stirred, the solution was reduced in volume and complex **6a** was crystallized by gas-phase diffusion of diethyl ether in a dichloromethane solution of **6a**. Yield: 122 mg (88%), red crystals. ^{1}H NMR ($CDCl_3$): δ 7.31 (m, 4 H, Ph-*H*), 7.27 (m, 8 H, Ph-*H*), 6.82 (m, 8 H, Ph-*H*), 5.95 (s, 4 H, C*H*(CCH_3)$_2$), 5.87 (s, 8 H, C*H*(CCH_3)$_2$), 5.03 (s, 0.32 H, SCH_2), 4.83 (s, br, 4 H, B*H*), 3.13 (s, 7.68 H, SCH_2), 2.57 (s, 12 H, CH_3), 2.47 (s, 24 H, CH_3), 2.36 (s, 12 H, CH_3), 1.55 (s, 24 H, CH_3). ^{13}C NMR ($CDCl_3$): δ (major isomer) 237.5 (Mo*C*SCH_2), 220.2 (*C*O), 218.4 (Mo*C*SPd), 153.2, 150.8, 147.3, 145.5 (*C*CH_3), 134.1, 128.7, 128.6, 127.9 (Ph-*C*), 108.2, 106.8 (*C*H(CCH_3)$_2$), 40.6 (S*C*H_2), 15.6, 15.3, 13.2, 12.9 (*C*H_3). IR (CH_2Cl_2, cm^{-1}): ν 2039, 1976 (s, CO).

[{Tp′(CO)$_2$W-η^2-(BnS)CC(S)}$_4$Pd](BF$_4$)$_2$ 6b. The corresponding tungsten complex **6b** was synthesized by a method analogous to **6a** using 143 mg (0.2 mmol) **3b**. Yield: 142 mg (90%), red solid. ^{1}H NMR ($CDCl_3$): δ 7.25 (m, 4 H, Ph-*H*), 7.20 (m, 8 H, Ph-*H*), 6.77 (m, 8 H, Ph-*H*), 6.00 (s, 4 H, C*H*(CCH_3)$_2$), 5.90 (s, 8 H, C*H*(CCH_3)$_2$), 4.88 (s, 0.24 H, SCH_2), 4.76 (s, br, 4 H, B*H*), 3.08 (s, 7.76 H, SCH_2), 2.59 (s, 12 H, CH_3), 2.47 (s, 24 H, CH_3), 2.35 (s, 12 H, CH_3), 1.71 (s, 24 H, CH_3). ^{13}C NMR ($CDCl_3$): δ (major isomer) 227.2 (W*C*SCH_2), 217.3 (*C*O), 209.1 (W*C*SPd), 154.8, 153.0, 148.4, 146.3 (*C*CH_3), 135.2, 128.9, 128.8, 128.0 (Ph-*C*), 109.3, 107.6 (*C*H(CCH_3)$_2$), 40.4 (S*C*H_2), 16.2, 15.1, 13.2, 12.8 (*C*H_3). IR (CH_2Cl_2, cm^{-1}): ν 2027, 1955 (s, CO).

X-ray Crystallography. Crystallographic data and structure refinement parameters of complexes **1b**, **3a**, **4b**, and **6a** are summarized in the Supporting Information. Single crystals suitable for X-ray analysis were coated in hydrocarbon oil and mounted on a glass fiber. X-ray intensities were measured at 153 K (**1b**, **4b**)

Table 1. EPR Parameters of Molybdenum(I) Complexes

	g_{iso}	A_{iso}	g_1 (A_1)	g_2 (A_2)	g_3 (A_3)
2a	1.994	28.0	1.980 (41)	2.009 (18)	2.029 (33)
[Tp′Mo(PhCCPh)(CO)$_2$][24]	2.007	30.7	1.977	2.009	2.036
[(η^5-C_5Me_5)Mo(CO)-(PhCCPh)$_2$][26]	1.991	27.5			
[(η^5-C_5Me_5)Mo(PhCCPh)$_2$][26]	2.027		2.006 (10)	2.024 (−)	2.048 (14)
[Tp′Mo(NO)Cl(NC_5H_5)][25]	1.97	48.6			
[(η^6-$C_6H_3{}^tBu_3$)(η^7-C_7H_7)-Mo](PF$_6$)$_2$[27]			1.9710 (55)	2.0024 (10)	

Table 2. Bonding Parameters in Thio-Alkyne Complexes, Selected Bonds (Å) and Angles (deg)

	1b	**3a**	**4b**
M−C1	2.064(10)	2.143(4)	2.044(3)
M−C2	2.060(10)	2.020(3)	2.024(3)
M−C17			2.165(3)
M−C25		2.026(4)	1.974(3)
C1−C2	1.313(14)	1.332(5)	1.339(4)
C1−S1	1.701(11)	1.650(4)	1.711(3)
C2−S2	1.706(11)	1.678(4)	1.701(3)
C1−C2−S2	139.1(9)	132.9(3)	134.8(2)
C2−C1−S1	141.7(8)	146.3(3)	141.4(3)

Table 3. CO Stretching Frequencies and Peak Potentials of Thio-Alkyne Complexes

	ν (CO, cm^{-1})	$E_{p,c}$ vs [Fc/Fc$^+$]	$E_{p,a}$ vs [Fc/Fc$^+$]
3a	2013, 1942	−1.54	0.55
[Ni(**3a**)$_4$](BF$_4$)$_2$ **5a**	2038, 1976	−0.87, −1.56	
[Pd(**3a**)$_4$](BF$_4$)$_2$ **6a**	2039, 1976	−1.07, −1.37, −1.53	
3b	2004, 1925	−1.69	0.53
[Ni(**3b**)$_4$](BF$_4$)$_2$ **5b**	2027, 1955	−1.05, −1.71	
[Pd(**3b**)$_4$](BF$_4$)$_2$ **6b**	2027, 1955	−1.29, −1.62	

and at 173 K (**3a**, **6a**) by using a Bruker AXS Apex system equipped with a rotating anode. All data were measured with Mo Kα radiation (λ = 0.71073 Å). Data collection, cell refinement, data reduction, and integration, as well as absorption correction, were performed with the Bruker AXS program packages SMART, SAINT, and SADABS. Crystal and space group symmetries were determined using the XPREP program. For further crystal and data collection details, see Table 4. All crystal structures were solved with SHELXS-97[20] by direct methods and were refined with SHELXL-97,[21] using anisotropic thermal parameters for all non-hydrogen atoms. The hydrogen atoms were included in the structure factor calculations at idealized positions. The PF_6 anion in **1b** is badly resolved and probably disordered. To obtain a stable refinement, we treated it as a fixed fragment. The F atoms share a common isotropic temperature factor.

Results and Discussion

Bis(benzylthio)acetylene Complexes. In the search for metal complex moieties with a strong alkyne binding ability in order to obtain robust complexes that can survive the aimed conversion reactions at the sulfur atoms, we found the Tp′M(CO)$_2$ complex fragments (M = Mo, W) particularly useful. Cationic alkyne complexes [Tp′M(CO)$_2$\{η^2-(BnS)CC(SBn)\}](PF$_6$) (M = Mo for **1a**, M = W for **1b**) have been synthesized by the straightforward method of Templeton[22] via oxidation of the 17-electron radical [Tp′M-(CO)$_3$] (M = Mo, W) with ferrocenium salts in the presence of bis(benzylthio)acetylene. Crystallization of the complexes from CH_2Cl_2/Et_2O yielded air-stable emerald **1a** and green **1b**. The ^{13}C NMR spectra of both compounds show alkyne resonances in the range of 194−227 ppm, which are typical for four-electron-donor alkyne complexes. Small changes of the benzylic CH_2 ^{13}C resonances of **1a**/**1b** compared with the free alkyne rule out coordination of the sulfide groups at the metal center. Evidence of neither intermediate coordination of the sulfide groups in solution nor corresponding byproducts could be observed (as described, for example,[10] for [(η^5-C_5H_5)Ru(PMe_3)$_2$(MeSCCSMe)]$^+$). IR spectroscopy indicates the fast and exclusive appearance of two carbonyl bands for one C_s symmetric complex species, displaying somewhat lower frequencies for **1b** (2041, 1980 cm^{-1}) because of the stronger π-back-bonding of tungsten. The molecular structure of **1b** (Figure 1) shows a roughly

Table 4. Crystallographic Data

	1b	**3a**	**4b**	**6a**
formula	$C_{33}H_{36}BF_6N_6O_2PS_2W$	$C_{33}H_{37}BMoN_6O_2S_2$	$C_{47}H_{50}BN_6O_2S_2W$	$C_{111}H_{133}B_6F_8Mo_4N_{24}O_9PdS_8$
fw	952.43	720.56	989.71	2910.91
cryst syst	hexagonal	triclinic	monoclinic	triclinic
space group	$R\bar{3}$	$P\bar{1}$	$P21$	$P\bar{1}$
a (Å)	21.64(2)	9.9460(10)	11.0754(5)	17.3601(13)
b (Å)	21.64(2)	11.8320(11)	17.8315(8)	18.2711(13)
c (Å)	46.42(6)	15.2025(15)	11.7455(6)	25.0020(18)
α (deg)	90.00	88.173(2)	90	93.194(2)
β (deg)	90.00	78.319(2)	108.4900(10)	109.147(2)
γ (deg)	120.00	79.183(2)	90	115.6360(10)
V (Å^3)	18825(34)	1720.8(3)	2199.89(18)	6570.0(8)
Z	18	2	2	2
ρ_{calcd} (g cm^{-3})	1.512	1.391	1.494	1.471
μ (mm^{-1})	2.962	0.541	2.766	0.706
$\lambda_{MoK\alpha}$ (Å)	0.71073	0.71073	0.71073	0.71073
T (K)	153	173(2)	153(1)	173(2)
no. of reflns collected	38 137	13 552	25 485	53 040
no. of unique reflns	5477	5960	12 324	23 137
R_{int}	12.54	4.62	2.48	9.20
no. of obsd reflns	4006	4926	11 744	12 371
F(000)	8496	744	1002	2966
R_1[a]	5.46	4.85	2.67	6.73
wR_2[b]	16.80	13.12	6.25	16.24
GOF	0.997	0.935	1.007	0.959
no. of params	448	460	539	1596

[a] Final R [$F > 2\sigma(F)$]. [b] R indices (all data).

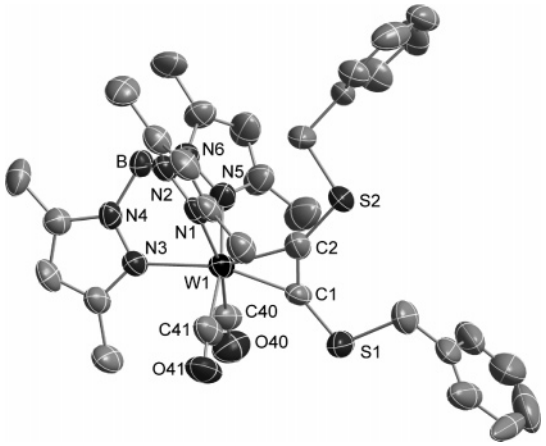

Figure 1. Molecular structure of the cation in **1b**. Hydrogens have been omitted for clarity.

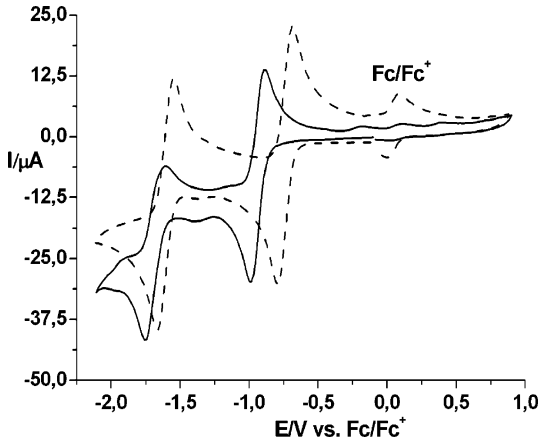

Figure 2. Cyclic voltammograms of **1a** (broken line) and **1b** (solid line) measured in CH_2Cl_2.

octahedral complex considering the alkyne as occupying a single coordination site. The M−C and C−C bond lengths are within the range of corresponding d^4 alkyne complexes bearing carbon substituents.[22] The alkyne C−C bond lengths of 1.317 Å and the strong bendback of the sulfur substituents from the C−C vector by 37 and 42° are consistent with a four-electron-donor alkyne complex. The alkyne SCCS plane lies between the carbonyl ligands approximately on the symmetry plane of the molecule. Fluxional behavior has not been observed in the room temperature ^{1}H NMR spectra of **1a**/**1b**. To evaluate the specific donor strength of sulfide-substituted alkynes by its influence on the CO frequencies, we used the approximation of Cotton and Kraihanzel.[23] A comparison of the CO force constants of **1b** (16.33 N cm^{-1}) with the corresponding tungsten complexes with 2-butine[22] (16.39 N cm^{-1}) and with diphenylacetylene[22] (16.45 N cm^{-1}) led to the finding that the nucleophilicity of the alkyne ligand increases with the substitution of phenyl by methyl groups and, to a similar extent, the substitution of methyl by benzylthio groups.

Reduction of the Bis(benzylthio)acetylene Complexes. Reductive removal of benzyl groups is a standard reaction in thiol protection chemistry. However, the alkyne sulfide functions in **1a**/**1b** raise the question of whether the carbon sulfur bonds are selectively cleaved at the sp or at the sp^3 position. According to the cyclic voltammograms, **1a** and **1b** undergo two reduction steps (Figure 2). The first reduction is indicated by a reversible wave at −0.80 and −0.97 V, respectively, and the second step appears less reversible at −1.65 and −1.74 V, respectively (peak potentials referenced against ferrocene/ferrocenium hereafter). Tungsten complex **1b** is more difficult to reduce than molybdenum congener **1a**. The first step at moderate potential is assigned to the reduction of the metal center because of its reversibility. To confirm this perception, we carried out reduction of **1a**/**1b** in preparative scale in THF solution by the addition of 1 equiv of potassium graphite (Scheme 1). The products **3a**/**3b**, which could be crystallized from red-brown toluene solutions, displayed puzzling ^{1}H NMR spectra with broad benzyl resonances. The X-ray structure analysis of **3a** and

Scheme 1. Synthesis of the Thio-Alkyne Complexes **3a**/**3b** and **4b**

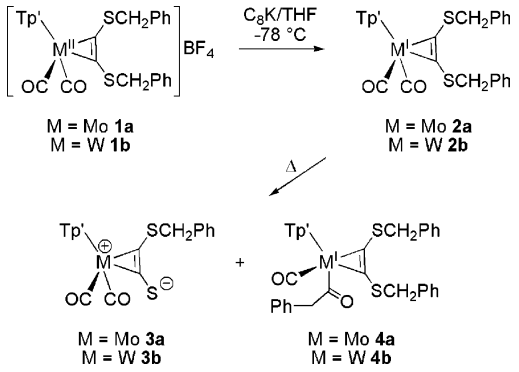

3b[14] disclosed the intended cleavage of one benzyl group in **1a**/**1b** and the identity of **3a**/**3b** as thio-alkyne complexes (Figure 5). This reactivity is remarkable with regard to the stability of the corresponding tolane complex [Tp′Mo(CO)$_2$-(η^2-PhCCPh)], which was described by Connelly and Orpen.[24]

To get insights into the reaction mechanism, we monitored the reduction process by IR spectroscopy using the CO stretching frequencies as a probe (Figure 3). Immediately after addition of C_8K to tungsten complex **1b**, a red reaction solution formed; at −78 °C, the solution displayed two markedly low-energy-shifted CO bands at 1959 and 1861 cm^{-1}. These bands are assigned to the intermediate complex **2b** with an electron-rich metal center (Scheme 1). In the course of 1 h at ambient temperature, the conversion of **2b** to **3b** is indicated by the appearance of a new pair of bands at 1996 and 1926 cm^{-1}. The CO stretching frequencies of **3b** reveal a loss of electron density at the metal compared to the intermediate **2b**. These observations, supported by the cyclic voltammograms of **1a**/**1b**, point to a mechanism in

(20) Sheldrick, G. M. *SHELXS-97: Program for Crystal Structure Solution*; Universität Göttingen: Göttingen, Germany, 1986−1997.
(21) Sheldrick, G. M. *SHELXL-97: Program for Crystal Structure Refinement*; Universität Göttingen: Göttingen, Germany, 1997.
(22) Feng, S. G.; Philipp, C. C.; Gamble, A. S.; White, P. S.; Templeton, J. L. *Organometallics* **1991**, *10*, 3504−3512.
(23) Cotton, F. A.; Kraihanzel, C. S. *J. Am. Chem. Soc.* **1962**, *84*, 4432−4438.
(24) Bartlett, I. M.; Connelly, N. G.; Orpen, A. G.; Quayle, M. J.; Rankin, J. C. *J. Chem. Soc., Chem. Commun.* **1996**, 2583−2584.

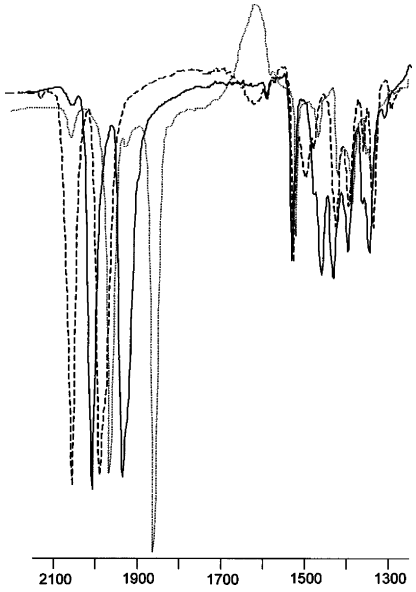

Figure 3. CO stretching frequencies of **1b** (broken line), **2b** (dotted line), and **3b** (solid line).

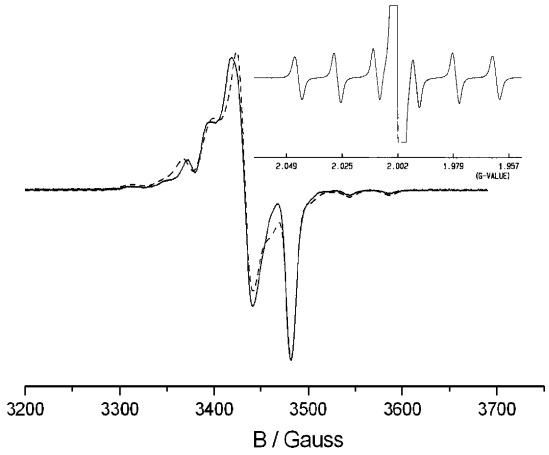

Figure 4. EPR spectra of **2a** in a frozen THF solution (measured, solid line; calculated, broken line) and at room temperature (inset).

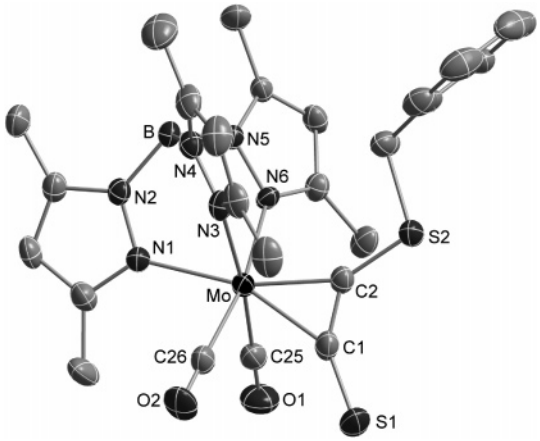

Figure 5. Molecular structure of **3a**. Hydrogens have been omitted for clarity.

which the metal center is reduced primarily in a fast step and the benzyl group is cleaved in a subsequent slower process. Thereby, the obvious removal of a benzyl radical at one sulfide function involves a transfer of metal-based electron density to the thio-alkyne unit, which is evident by the medium CO frequencies of **3a**/**3b** compared to those of **1a**/**1b** and **2a**/**2b**, respectively. The cleavage of the benzyl group proceeds much slower with the molybdenum system, which is surprising at a first glance because of the usually higher reactivity of molybdenum complexes. However, the cleavage is presumably promoted by the higher electron density at tungsten.

The first metal-directed reduction step could be unequivocally proven by EPR spectroscopy (Figure 4). The room-temperature EPR spectrum of **2a** displays an isotropic signal with a clearly resolved hyperfine coupling to $I = 5/2$ isotopes (^{95}Mo (15.9%) and ^{97}Mo (9.6%)). This observation points to Mo(I) intermediate **2a**, in which the unpaired electron is predominantly localized at the metal. In a frozen solution, a rhombic g-tensor is apparent from the low-temperature spectrum at X-band frequency. In addition, a simulation of the spectrum provides hyperfine coupling values with pronounced anisotropy. The average of the three anisotropic A values agrees well with the isotropic value A_{iso} observed in the room-temperature spectrum. The hyperfine coupling constants, which are summarized and related to literature data in Table 1, are rather small compared to innocent paramagnetic molybdenum complexes. Comprising Mo(I) d^5 complexes, the A values of **2a** are distinctively smaller compared to those of [Tp′Mo(NO)Cl(pyridine)][25] but higher compared to those of alkyne complex [Cp*Mo(η^2-PhCCPh)$_2$][26] with a predominantly ligand-based SOMO. This observation can be rationalized with some delocalization of the unpaired electron into the coordinated alkyne, which is reflected by the uncovered reactivity. The accordance of the g and A values of [Tp′Mo(CO)$_2$(η^2-PhCCPh)][24] with **2a** is notable, the latter of which is furnished with just the weak S−C$_{benzyl}$ bond.

With the intention of increasing the yields of products **3a**/**3b**, the mother liquors of crystallization attempts were subjected to chromatographic purification. Thereby, we isolated a byproduct **4b** in a surprisingly high yield that is comparable to the yield of **3b**. Tungsten complex **4b** could be isolated in substance and fully characterized, whereas corresponding molybdenum complex **4a** turned out to be unstable. The ^{1}H NMR spectrum of diamagnetic compound **4b** displays six nonequivalent CH*H* protons that represent three different benzyl groups in a chiral metal complex. The identity of **4b** could be resolved by X-ray structure analysis (Figure 6). The molecular structure of **4b** disclosed the fate of the benzyl radical in the cleavage reaction, because the tungsten center is coordinated beside the Tp′ and one CO ligand by the still-intact alkyne and one acyl group. The cleaved benzyl radicals do not simply recombine but attack, preferably, another molecule of **2b** in terms of an alternative combination of radicals.

Further mechanistic evidence was sought from kinetic investigations on the basis of UV−vis spectroscopic monitoring of the cleavage reaction with molybdenum complex

(25) McWhinnie, S. L.; Jones, C. J.; McCleverty, J. A.; Collison, D.; Mabbs, F. E. *J. Chem. Soc., Chem. Commun.* **1990**, 940−942.
(26) Connelly, N. G.; Geiger, W. E.; Lovelace, S. R.; Metz, B.; Paget, T. J.; Winter, R. *Organometallics* **1999**, *18*, 3201−3207.

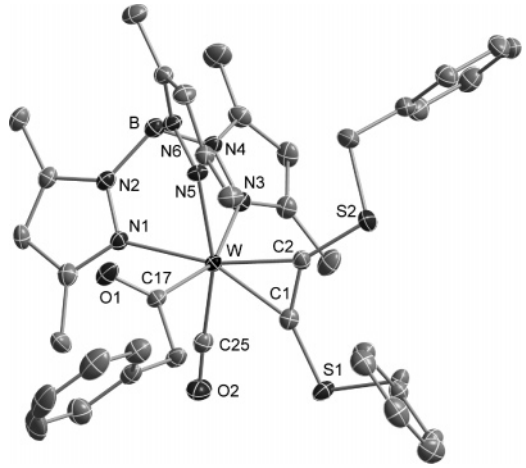

Figure 6. Molecular structure of **4b**. Hydrogens have been omitted for clarity.

2a. The observation of isosbestic points led to the assumption of a bimolecular mechanism. However, an initial rate vs start concentration correlation was found to be linear, which does not support a bimolecular mechanism. The first-order kinetics for the overall consumption of starting material **2a** can be rationalized by the assumption of parallel reactions with a steady-state concentration of the benzyl radical. The radical attack is so fast relative to the comparatively slow cleavage reaction (the half-life of **2a** at room-temperature falls in the dimension of days) that the sum reaction 2 (**2a**) → **3a** + **4a**, becomes apparent by the observation of isosbestic points in the UV−vis monitoring.

Molecular Structures of 3a and 4b. The overall complex structure of **3a** (Figure 5) resembles the structure of corresponding cationic tungsten complex **1b**. Considering the thioalkyne ligand as occupying a single coordination site, **3a** exhibits a roughly octahedral complex polyhedron. The thioalkyne moiety in **3a** is coordinated in a η^2-*CC* fashion with a free terminal sulfur atom, as already found in corresponding complexes obtained by C−C bond formation in the complex.[12,13] The difference of the C1−C2 bond lengths between **1b** and **3a** (1.332 Å; see Table 2) is within the margin of error. The SCCS plane likewise lies approximately on the symmetry plane of the molecule. The terminal sulfur atom adopts a syn position with respect to the carbonyl ligands. The direct comparison of the C_{sp}−S bond lengths to the sulfide group (1.678 Å) and to the terminal sulfur atom (1.650 Å) in an individual molecule of **3a** discloses little double-bond character for the C1−S1 bond when applying the bond-length criteria. However, according to resonance structure **A**, the thioketenyl character is evident by the distinctly shorter Mo−C2 bond (2.020 Å) compared with that of Mo−C1 (2.143 Å). Interestingly, stable thioketenes form either η^1-*S* or η^2-*SC* complexes.[28,29]

With regard to the rotation of the η^2-*C,C*-bound ligand at the metal center, **3a**/**3b** behave in solution like typical alkyne complexes.[30] In the ^{1}H NMR spectrum of **3a** at −60 °C, two CH_2 resonances at 5.20 and 3.26 ppm exhibit comparable intensity. The high-field-shifted signal is assigned to the isomer found in the crystal, because NOE experiments disclose proximity of the CH_2 protons to the pyrazole pocket. A double signal set is consistently observed in the ^{13}C NMR spectrum at −60 °C, and the correct assignment of the alkyne carbon resonances for both rotational isomers has been done by correlation of the Ph*C*H_2 resonance pair with the low-field-shifted alkyne *C* pair in a gHMBC spectrum. The free activation enthalpies ΔG^*_{298} of the rotation between the syn and the anti positions of the terminal sulfur regarding the carbonyl ligands have been determined to be 60.5 kJ/mol (**3a**) and 58.3 kJ/mol (**3b**) by line-shape analysis of the variable temperature ^{1}H NMR spectra (see the Supporting Information, Figures S1 and S2).

The molecular structure of **4b** (Figure 6) is interesting because of its correlation to **1b**. The tungsten(II) center in **4b** bears one acyl ligand in substitution for one CO, and complex **4b** is consequently neutral in contrast to cationic **1b**. Considering the alkyne ligand again as occupying a single coordination site, **4b** likewise shows a roughly octahedral structure. However, the C_2S_2 alkyne plane does not bisect the C_3 symmetric Tp′ ligand; it is aligned with the residual CO ligand. Compared with those of **1b**, the W−C1 and W−C2 bonds (2.024 and 2.044 Å, respectively) are somewhat shorter and the C1−C2 distance (1.339 Å) is slightly longer. The W−N bond lengths increase in the order W−N5, W−N3, and W−N1, which correspond to the trans position of CO, acyl function, and alkyne ligand, respectively. The W−C17 bond of the acyl group displays the longest tungsten carbon bond in **4b** (2.165 Å), which falls at the shorter limit for tungsten η^1-acyl complexes.[31−33] Comparison of **4b** with related alkyne complex [Tp′Mo(CO)$_2$(η^2-PhCCPh)][24] is instructive, because the reduction of [Tp′Mo(CO)$_2$(η^2-PhC-CPh)]$^+$ by one electron induces a decrease in the C−C bond length and an elongation of the metal−carbon bonds. The opposite is observed for the cationic **1b** and neutral **4b** pair, because in this case, the electron density at molybdenum increases without a change in the oxidation state. With regard to Tp compounds of group VI metals, predominantly η^2-acyl complexes with distinctively shorter M−C bonds are known.[34−36] The η^2-alkyne−η^1-acyl binding mode of **4b** has already been found in [Tp′W(CO){ η^2-MeCCPh}{C(O)-Bu}].[37] Corresponding molybdenum complexes have solely

(27) Beddoes, R. L.; Elwell, M. S.; Mabbs, F. E.; McInnes, E. J. L.; Roberts, A.; Sarwar, M. F.; Whiteley, M. W. *J. Chem. Soc., Dalton Trans.* **2000**, 4669−4676.
(28) Wormsbächer, D.; Edelmann, F.; Behrens, U. *Chem. Ber.* **1982**, *115*, 1332−1338.
(29) Werner, H.; Kolb, O.; Schubert, U.; Ackermann, K. *Chem. Ber.* **1985**, *118*, 873−879.
(30) Templeton, J. L. *Adv. Organomet. Chem.* **1989**, *29*, 44−61.
(31) Adams, H.; Bailey, N. A.; Tattershall, C. E.; Winter, M. J. *J. Chem. Soc., Chem. Commun.* **1991**, 912−914.
(32) Chen, J.-D.; Wu, C.-K.; Wu, I.-Y.; Huang, B.-C.; Lin, Y.-C.; Wang, Y. *J. Organomet. Chem.* **1993**, *454*, 173−181.
(33) Sakaba, H.; Tsukamoto, M.; Kabuto, C.; Horino, H. *Chem. Lett.* **2000**, 1404−1405.
(34) Curtis, M. D.; Shiu, K.-B.; Butler, W. M. *J. Am. Chem. Soc.* **1986**, *108*, 1550−1561.
(35) Rusik, C. A.; Collins, M. A.; Gamble, A. S.; Tonker, T. L.; Templeton, J. L. *J. Am. Chem. Soc.* **1989**, *111*, 2550−2560.
(36) Stone, K. C.; Onwuzurike, A.; White, P. S.; Templeton, J. L. *Organometallics* **2004**, *23*, 4255−4264.
(37) Feng, S. G.; Templeton, J. L. *Organometallics* **1992**, *11*, 2168−2175.

Scheme 2. Synthesis of the Heterobimetallic Complexes of **3a**/**3b** with Ni(II) and Pd(II)

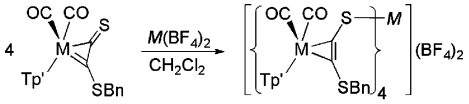

M = Mo **3a**
M = W **3b**

M = Ni, M = Mo **5a**
M = Ni, M = W **5b**
M = Pd, M = Mo **6a**
M = Pd, M = W **6b**

been discussed as intermediates in the C−C bond formation between alkynes and η^2-bound acyl groups in the complex.[35] This reactivity, investigated by Templeton, provides a rationale for the difficulties in isolating the molybdenum analogue of **4b**.

Complex Formation of 3a/3b with Ni(II) and Pd(II). To explore the coordination behavior of thio-alkyne complexes, we reacted **3a**/**3b** with $[Ni(CH_3CN)_6](BF_4)_2$ and $[Pd(CH_3CN)_4](BF_4)_2$ in CH_2Cl_2 (Scheme 2). The immediate complex formation is indicated by a distinct increase in the CO stretching frequencies in the IR spectrum ($\Delta\nu$(**3a**) = 34 and 25 cm^{-1}, $\Delta\nu$(**3b**) = 30 and 23 cm^{-1}). Independent from the equivalents of **3a**/**3b** used in the synthesis, the tetracoordinated complexes $[Ni(\mathbf{3a})_4](BF_4)_2$ **5a**, $[Ni(\mathbf{3b})_4](BF_4)_2$ **5b**, $[Pd(\mathbf{3a})_4](BF_4)_2$ **6a**, and $[Pd(\mathbf{3b})_4](BF_4)_2$ **6b** are obtained after crystallization from *n*-hexane/CH_2Cl_2, according to ESI-mass spectroscopy. ^{13}C NMR spectroscopy discloses that the sulfide groups do not take part in the coordination. Regarding the rotational isomerism in the alkyne complex, the isomer with the terminal sulfur atom in proximity to the CO ligands prevails either absolutely (**5a**/**5b**) or extremely (**6a**/**6b**), as indicated by ^1H NMR spectroscopy. The effect of the sulfur coordination with nickel and palladium at the tungsten and molybdenum alkyne moiety, respectively, can be estimated by comparison of the CO frequencies in the IR spectra (Table 3) and the alkyne ^{13}C NMR shifts. The CO vibrations at molybdenum and tungsten show approximately 70% compensation of the original low-frequency shift from cationic **1a**/**1b** to neutral **3a**/**3b**. The increase in the CO frequencies reveals an enhanced positive partial charge at the group VI metal centers, which is affected by the sulfur coordination with nickel and palladium.

The difference between the two alkyne carbon resonances in the ^{13}C NMR spectra changes distinctly from **1a** ($\Delta\delta$ = 11.6) to **3a** ($\Delta\delta$ = 30.4) and finally to **5a** ($\Delta\delta$ = 21.1). Generally, this observation corroborates the thioketenyl complex character of **3a**. Interestingly, the high-field shift upon coordination of **3a** at nickel is larger for C2 ($\Delta\delta$ = 15.2) than for C1 ($\Delta\delta$ = 3.9). The stronger effect on C2, which is only indirectly affected by the coordination of nickel at the sulfur attached to C1, can be understood by the decrease in the Mo−C2 double-bond character. The π-back-bonding of molybdenum in **3a** is primarily directed at C2, which is reflected by the double bond in thioketenyl complex resonance form **A**. This effect is reduced in **5a**, because the electron-withdrawing effect of the LEWIS acid Ni^{2+} causes a more-balanced ratio of π-back-bonding to both C1 and C2. The reduced π-back-bonding to C2 in turn decreases the σ-donation, which is indicated by the observed high-field shift in the ^{13}C NMR spectrum. These changes are less-pronounced for the tungsten congeners, possibly because of the stronger π-back-bonding capacity of tungsten.

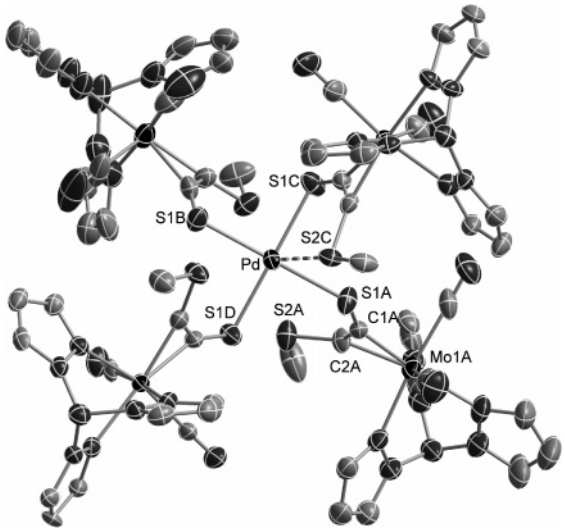

Figure 7. Molecular structure of the cation in **6a**. Hydrogen atoms and methyl and phenyl groups have been omitted for clarity. Selected bonds (Å) and angles (deg): Pd−S1A 2.334(2), Pd−S1B 2.313(2), Pd−S1C 2.347(2), Pd−S1D 2.320(2), Mo1A−C1A 2.074(7), Mo1A−C2A 2.041(7), C1A−C2A 1.341(9), C1A−S1A 1.659(8), C2A−S2A 1.647(7); S1A−Pd−S1C 90.41(6), S1A−Pd−S1D 90.27(5), S1B−Pd−S1C 90.02(6), S1B−Pd−S1D 90.03(5), S1A−Pd−S1B 171.32(5), S1C−Pd−S1D 175.18(5), Pd−S1A−C1A 110.0(3), S1A−C1A−C2A 145.3(6).

The identity of $[Pd(\mathbf{3a})_4](BF_4)_2$ **6a** has been unambiguously confirmed by X-ray structure analysis (Figure 7). The entire complex cation is crystallographically independent, rendering the variable number comparatively high. The central palladium is distorted square planar coordinated with Pd−S1 bonds ranging from 2.313 to 2.347 Å, which are typical for Pd(II) complexes with neutral thioketo donors.[38−41] The molybdenum complex moieties in trans position are tilted to the same side of the central square unit, obviously releasing the sterical crowding. Whereas the Mo−C2 bonds (average 2.023 Å) are comparable with those of the metallaligand **3a**, the Mo−C1 bonds (average 2.078 Å) are remarkably shorter and resemble instead the corresponding value in **1b**. The carbon−sulfur bonds (C1−S1 average, 1.661 Å; C2−S2 average, 1.667 Å) are equal within the margin of error. Tetracoordinated complexes of Pd(II) with neutral thioketo ligands such as thiourea derivatives or pyridinium-2-thione show frequently weak coordination of the counterions at the apical positions.[38−41] In **6a**, one of the palladium sulfide distances is notably shorter (Pd−S2C, 3.543 Å) than the other three, which leads to the longest Pd−S1 bond (Pd−S1C, 2.347 Å) and the smallest Pd−S1−C1 angle (Pd−S1C−C1C, 103.7°). However, even the Pd−S2C bond length just coincides with the sum of the van der Waals radii.[42]

(38) Berta, D. A.; Spofford, W. A.; Boldrini, P.; Amma, E. L. *Inorg. Chem.* **1970**, *9*, 136−142.
(39) Butler, L. M.; Creighton, J. R.; Oughtred, R. E.; Raper, E. S.; Nowell, I. E. *Inorg. Chim. Acta* **1983**, *75*, 149−154.
(40) Umakoshi, K.; Ichimura, A.; Kinoshita, I.; Ooi, S. *Inorg. Chem.* **1990**, *29*, 4005−4010.
(41) Vilar, R.; Mingos, D. M. P.; White, A. J. P.; Williams, D. J. *Chem. Commun.* **1999**, 229−230.

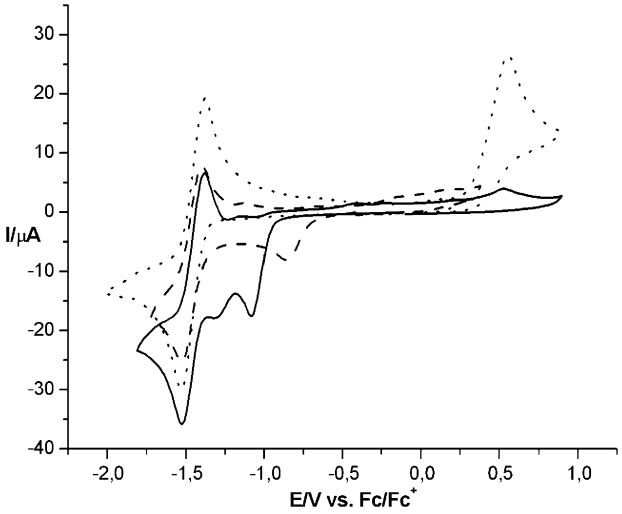

Figure 8. Cyclic voltammograms of **3a** (dotted line), **5a** (broken line), and **6a** (line) measured in CH_2Cl_2 solution with a scan rate of 100 mV s^{-1}.

The redox responsivity of the group VI metals for the coordination of the sulfur donor with nickel and palladium has been investigated by cyclic voltammetry (Figure 8). The metallaligands **3a**/**3b** undergo a reversible electron transfer at $E_{p,c} = -1.54$ for **3a** and $E_{p,c} = -1.69$ V for **3b**. The coordination of **3a**/**3b** to nickel and palladium leads to a remarkable positive shift in the first reduction potentials. The CV of **6a** exemplarily displays three successive reduction waves. The first two are irreversible; the third is quasireversible and represents an electron transfer at a potential comparable to that of free metallaligand **3a**. The CVs of the nickel complexes show only one broad irreversible reduction wave and a quasireversible signal at approximately −1.5 V. An unequivocal assignment of the reductions seems difficult. However, the first reduction step can presumably be attributed to the group VI metal centers for the following reasons. The peak potentials of the first reduction wave of **3a**/**3b**, **5a**/**5b**, and **6a**/**6b** (measured at invariable sweep rates of 100 mV s^{-1}) are in a reasonable linear relationship with the force constants of the CO ligands at molybdenum and tungsten (see the Supporting Information, Figure S11). The potential difference between Mo complex **3a** and its W congener **3b** is even increased within both the nickel and the palladium complexes, with nickel compounds **5a**/**5b** being easier to reduce. However, the irreversibility of the first reduction process is even observed, if the potential sweep is confined to this process (see the Supporting Information, Figure S12). A plausible explanation for this behavior implies a fast intramolecular electron transfer to the central metal ion. This interpretation is corroborated by reduction experiments in preparative scale. If the nickel and palladium complexes are reduced by 2 equiv of cobaltocene in CH_2Cl_2 (**5a**/**5b**) or THF (**6a**/**6b**), the release of ligands **3a**/**3b** is observed, according to IR and UV−vis spectroscopic evidence. Hence, the released ligands **3a**/**3b** give rise to the quasireversible signal in the CVs of the heterobimetallic complexes **5a**/**5b** and **6a**/**6b** at −1.5 V. Additional evidence of the ligand release after the first reduction step is uncovered

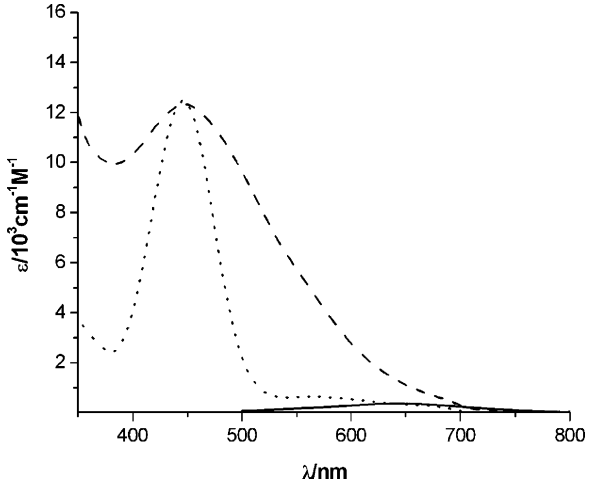

Figure 9. UV−vis spectra of **5b** in CH_2Cl_2 (broken line), **5b** in 1% THF in CH_2Cl_2 (dotted line), and $[Ni(tmtu)_4](BF_4)_2$ (line).

in the anodic part of the CVs. Metalla-ligands **3a**/**3b** show an oxidation wave at approximately 0.54 V that is assigned to the disulfide formation. This electron transfer is reasonably not observed in the CV of heteronuclear complexes **6a**/**6b**, if the potential sweep is started at 0 V with the oxidation. However, the oxidation wave at 0.54 V is observed in the reverse sweep mode, indicating the existence of free ligand in solution after the reduction (see the Supporting Information, Figure S13).

Surprisingly, nickel complexes **5a**/**5b** turned out to be unstable in donor solvents such as THF and CH_3CN, because these solvents compete as ligands. In contrast to **6a**/**6b** and according to ^{1}H NMR and IR spectroscopic data, THF solutions of **5a**/**5b** contain predominantly free ligands **3a**/**3b**. The UV−vis spectrum of intensely red **5b** is dominated by the charge-transfer band of the tungsten complex moiety (Figure 9). The nickel-based transition is probably obscured, as indicated by comparison with the UV−vis spectrum of green $[Ni(tmtu)_4](BF_4)_2$ (tmtu = tetramethylthiourea). Interestingly, the release of **3b** is more evident by the sharpening of the tungsten-based charge-transfer band than by an energy shift. Possibly the solution structure of **5b** adopts a low symmetry comparable to the solid-state structure of **6a**. Such a low-symmetry structure must be fluxional in the NMR time scale, because the corresponding spectra display 4 equiv **3b** ligands. Alternatively, the broadening of the band in **5b** can be attributed to the electronic interaction of the four chromophores over the central metal ion. The ESI mass spectrum of **5b** in THF solution shows a number of diverse species such as $[Ni(\mathbf{3b})_3]^{2+}$, $[Ni(\mathbf{3b})_2(THF)]^{2+}$, and $[Ni(\mathbf{3b})(THF)_5]^{2+}$. We are currently exploring possibilities for activating substrates at nickel complex ions in CH_2Cl_2/THF solvent mixtures.

Conclusion

The goal of the work described in this contribution was to access heterobimetallic complexes featuring η^2-*C*,*C*−η^1-*S* alkyne−thiolate linkers. Our approach, comprising primary formation of alkyne complexes with suitable acetylenedisulfides, subsequent removal of the sulfur protection groups,

(42) Bondi, A. *J. Phys. Chem.* **1964**, *68*, 441−451.

and final complex formation with thiophilic transition-metal ions, turned out to be generally successful. The η^2-alkyne complexes of bis(benzylthioacetylene) with d^4 metal complex fragments $Tp'M(CO)_2$ (M = Mo, W) are sufficiently robust to allow necessary conversions at the sulfur atom. The resulting thio-alkyne complexes with one terminal sulfur donor have been proven in turn to act as metallaligands, which form homoleptic Werner type complexes with Ni(II) and Pd(II). The structural, electrochemical, and IR spectroscopic data reveal a partially zwitterionic nature of the metallaligands in these pentanuclear complexes. This charge transfer into the alkyne complexes is emphasized in a resonance structure with two cationic peripheral alkyne complex moieties and a neutral complex core. The reactivity of the heterobimetallic complexes in donor solvents and redox reactions discloses a high electronic flexibility of the metallaligands. Pentanuclear heterobimetallic complexes of type **5a**/**5b** and **6a**/**6b** seem promising, because the generally redox-active alkyne complex moieties might be able to deliver up to four electrons to a potential substrate coordinated at the central metal ion (e.g., in the apical position). In this context, further work is directed toward less-noble central metal ions, such as Fe(II).

Acknowledgment. The Deutsche Forschungsgemeinschaft is gratefully acknowledged for financial support of this work. W.W.S. thanks Prof. F. E. Hahn for generous support and Dr. E. Bill (MPI Mülheim) for the EPR measurements.

Supporting Information Available: Variable-temperature ^{1}H NMR spectra of **3a**; Eyring plot and activation parameters for **3a** and **3b** obtained by line shape analysis; kinetic data for the conversion of **2a** to **3a**; NMR spectra of **5a**/**5b** and **6a**/**6b**; additional CV data of **5a**/**5b** and **6a**, crystallographic information files for **1b**, **3a**, **4b**, and **6a**. This material is available free of charge via the Internet at http://pubs.acs.org.

IC052178Y